J. Fluid Mech. (1982), *vol.* 118, *pp.* 315–339
Printed in Great Britain

Anisotropic modelling of thermal convection in multilayered porous media

By ROBERT McKIBBIN
Department of Theoretical and Applied Mechanics,
University of Auckland, New Zealand
AND PEDER A. TYVAND
Department of Mechanics, University of Oslo, Norway

(Received 1 December 1980 and in revised form 18 May 1981)

The principle of large-scale anisotropy due to small-scale layering is applied to thermal convection. The motion takes place in a bounded porous medium heated from below. The medium is periodically layered with respect to permeability and thermal conductivity. The onset of convection as well as slightly supercritical convection are investigated. Anisotropic modelling proves useful even for small numbers of layers as long as the motion is of 'large-scale convection' type (Masuoka *et al.* 1978). The modelling always fails for motion of 'local convection' type.

1. Introduction

A correspondence between layering and anisotropy is encountered in a broad class of physical problems. Most familiar, perhaps, is the basic anisotropy effect of layering in electric conduction (series and parallel arrangements of resistors). Also, elastic and electromagnetic waves in layered media propagate as if the media were anisotropic when the wavelength is sufficiently large compared to the layer thicknesses (see e.g. Brekhovskikh 1960, p. 79). Heat conduction and other transport phenomena may also exhibit these features.

A layered porous medium can, under certain circumstances, be represented by an anisotropic model medium. For example, Marcus & Evenson (1961) showed by considering uniform flows (i.e. uniform flows in each layer) that the set of scalar layer permeabilities of a multilayered medium is macroscopically equivalent to an average permeability tensor (see also Bear 1972, p. 157; Wooding 1976). Anisotropic modelling has also been applied to hydrodynamic dispersion (Moranville, Kessler & Greenkorn 1977*a*, *b*; Tyvand 1980) for the case of uniform flows through porous media.

The anisotropic representation is also relevant, however, for a curved flow in a layered porous medium when the length scale of the flow is sufficiently large compared to the layer thicknesses. The primary purpose of the present work is to investigate the ability of an average anisotropic model to represent curved flows in layered systems. As a mathematically convenient and illustrative family of flows, free thermal convection is considered. This has considerable geophysical and technical importance (see Combarnous & Bories 1975; Cheng 1978). Layering in both permeability and thermal conductivity are investigated.

The criterion for onset of two-dimensional convection in a porous medium com-

posed of two layers has recently been studied by Masuoka *et al.* (1978), who also investigated supercritical flow patterns using a finite-difference method. McKibbin & O'Sullivan (1980) developed a general method for analysing a medium composed of an arbitrary number of separately homogeneous layers and this method is followed here. In this paper some aspects of nonlinear convection are also studied, following McKibbin & O'Sullivan (1981).

It was found, in the last three studies mentioned, that convection tends to localize in those layers which have greater permeability (see also Ribando & Torrance 1976). This 'local' convection is also associated with motion of a fluid whose viscosity decreases with increasing temperature – relatively large flow rates occur near the hot bottom of the system (see e.g. Zebib & Kassoy 1977). In a homogeneous layer saturated with a constant-viscosity fluid, however, local convection does not occur, the flow being of 'large-scale' type. Among other relevant works on convection in non-homogeneous porous media are those by Donaldson (1962) and Green & Freehill (1969).

The theory of convection in homogeneous anisotropic porous media was first considered by Castinel & Combarnous (1974) and Epherre (1975), who found onset criteria for systems which have an impermeable upper boundary. Kvernvold & Tyvand (1979) extended these analyses to supercritical finite-amplitude convection. Wooding (1976) presented criteria for onset of two- and three-dimensional convection in a layer with permeability that is anisotropic and which may also vary with depth – both impermeable and constant-pressure upper-boundary conditions were treated.

The present study extends the theory of convection in layered and anisotropic porous media and provides a link between these two fields.

2. The multilayered porous medium

As previously analysed by McKibbin & O'Sullivan (1980, 1981), the multilayered system, of total thickness d, is assumed to comprise N separately homogeneous isotropic layers. Beneath layer 1 the system is bounded by an impermeable isothermal surface at temperature $T_a + \Delta T$, where T_a is the temperature of the isothermal top surface (above layer N) which is considered to be either impermeable (closed top) or at constant pressure (open top). The porous material contained in layer i, of thickness d_i, has permeability K_i, and, when saturated, thermal conductivity k_i. Within each layer the usual equations of conservation of mass, momentum (Darcy's law) and energy hold. Appropriate continuity considerations determine boundary conditions at the interfaces between the layers.

The conduction solution for the temperature T_s is a piecewise linear function of the vertical co-ordinate z, given by

$$T_s = T_a + \Delta T \left(\sum_{j=i}^{N} \delta_j - \frac{z - z_{i-1}}{k_i} \right) \Big/ \delta, \tag{2.1}$$

for $z_{i-1} < z < z_i$, where

$$z_i = \sum_{j=1}^{i} d_j \quad \text{and} \quad \delta_i = d_i/k_i, \quad \delta = \sum_{j=1}^{N} \delta_j.$$

This distribution corresponds to a temperature drop ΔT_i across each layer given by

$$\Delta T_i = \frac{\delta_i}{\delta} \Delta T. \tag{2.2}$$

It should be noted that, when the layer conductivities are all the same (i.e. $k_i = k_1$, $i = 2, 3, \ldots, N$) the conduction-temperature distribution is the same as that for a homogeneous layer, viz. $T_s = T_a + \Delta T(1 - z/d)$ for $0 < z < d$, with a temperature drop across each layer proportional to the fraction $r_i (= d_i/d)$ of the total thickness that the layer occupies, namely $\Delta T_i = r_i \Delta T$.

In the general case, a Rayleigh number for each layer, based on the layer thickness d_i and the layer temperature drop ΔT_i is given by

$$R_i = \frac{\rho_a g c \alpha K_i d_i \Delta T_i}{\nu k_i}, \tag{2.3}$$

where ρ_a, c, α and ν are respectively the density at temperature T_a, the thermal-expansion coefficient, the specific heat and the kinematic viscosity of the saturating fluid, and g is the acceleration due to gravity.

Each layer Rayleigh number may be related to that for the bottom stratum, layer 1, by

$$\frac{R_i}{R_1} = \frac{K_i d_i^2}{k_i^2} \frac{k_1^2}{K_1 d_1^2}. \tag{2.4}$$

The criterion for onset of convection in such a multilayered system becomes an eigenvalue problem which is solved (see McKibbin & O'Sullivan 1980) for the parameter R defined by

$$R = \frac{\delta d}{\delta_1 d_1} \frac{R_1}{4\pi^2} = \frac{\rho_a g c \alpha K_1 d \Delta T}{4\pi^2 \nu k_1}. \tag{2.5}$$

Calculation of the critical value $R = R_c$ enables a comparison to be made of the temperature difference required for onset of convection in the system, with that for an infinite layer which is composed completely of the material of layer 1 for the stratified case.

In order that comparison may be made with an 'equivalent' homogeneous anisotropic layer, the effective anisotropy of the stratified system must be found. By considering uniform flows parallel and perpendicular to the layering, average horizontal and vertical permeabilities and conductivities may be calculated. These are

$$\left.\begin{aligned} K_H &= \sum_{i=1}^{N} r_i K_i, \quad K_V = \left(\sum_{i=1}^{N} \frac{r_i}{K_i} \right)^{-1}, \\ k_H &= \sum_{i=1}^{N} r_i k_i, \quad k_V = \left(\sum_{i=1}^{N} \frac{r_i}{k_i} \right)^{-1}, \end{aligned}\right\} \tag{2.6}$$

where subscripts H, V denote horizontal and vertical parameters respectively, and $r_i = d_i/d$. A model of alternating layers will be the best analogy for a homogeneous medium. In what follows, then, the total number of layers N is even; a number $\frac{1}{2}N$ of superposed pairs of layers is considered, each pair being of total thickness $2d/N$ and comprising two layers of thicknesses $r(2d/N)$, $(1-r)(2d/N)$, with permeabilities K_1, βK_1 and conductivities k_1, γk_1 respectively. Average horizontal and vertical permeabilities and conductivities for the system are, using (2.6), given by

$$\left.\begin{aligned} \frac{K_H}{K_1} &= r + (1-r)\beta, \quad \frac{K_V}{K_1} = \left(r + \frac{1-r}{\beta} \right)^{-1}, \\ \frac{k_H}{k_1} &= r + (1-r)\gamma, \quad \frac{k_V}{k_1} = \left(r + \frac{1-r}{\gamma} \right)^{-1}. \end{aligned}\right\} \tag{2.7}$$

Measures of effective anisotropy in permeability and conductivity are then given by the parameters ξ, η respectively, where

$$\left.\begin{aligned}\xi &= \frac{K_H}{K_V} = [r+(1-r)\beta]\left[r+\frac{1-r}{\beta}\right],\\ \eta &= \frac{k_H}{k_V} = [r+(1-r)\gamma]\left[r+\frac{1-r}{\gamma}\right]\end{aligned}\right\} \tag{2.8}$$

Note that both ξ, $\eta > 1$ i.e. horizontally layered systems correspond to anisotropy only of a form where horizontal are larger than vertical quantities. Also the choice of N even leaves ξ, η independent of N (for an odd number of layers, ξ and η depend on N – however as N becomes large these values converge towards those in (2.8)).

Suitable choices of r, β and γ enable any desired values of ξ, $\eta > 1$ to be obtained, although it should be noted that to each value of ξ, for a given r, there correspond two values of β, namely β^+ (the larger value) and $\beta^- = 1/\beta^+$. These are given by

$$\beta^{\pm} = \frac{\xi-[r^2+(1-r)^2] \pm [(\xi-1)(\xi-(2r-1)^2)]^{\frac{1}{2}}}{2r(1-r)}. \tag{2.9}$$

There are similarly two possible values of $\gamma(\gamma^+, \gamma^- = 1/\gamma^+)$ for each chosen η. Towards the limit as ξ, $\eta \to \infty$,

$$\beta^+ \to \frac{\xi}{r(1-r)}, \quad \gamma^+ \to \frac{\eta}{r(1-r)},$$

with

$$\beta^- \to \frac{r(1-r)}{\xi}, \quad \gamma^- \to \frac{r(1-r)}{\eta}.$$

For given ξ, $\eta > 1$, there are thus four possible combinations of values of β, γ that may be chosen. For most of the cases studied below where one of ξ and η is unity, the smaller value γ^- or β^- respectively is chosen. For a closed-top system, where symmetry is preserved via the similar upper and lower boundary conditions, there will be no qualitative difference between subsequently calculated flows using either of the choices. For open-top systems, this symmetry is not preserved, and for small numbers of layers, the different selections give slightly different results. As N becomes large, however, the distinction tends to disappear.

A Rayleigh number R^* for the system may be defined in terms of the effective vertical permeability and conductivity, as

$$R^* = \frac{\rho_a g c \alpha K_V d \Delta T}{4\pi^2 \nu k_V}. \tag{2.10}$$

Upon using (2.7),

$$R^* = \frac{r+(1-r)/\gamma}{r+(1-r)/\beta} R, \tag{2.11}$$

where R is given by (2.5). The critical value of this Rayleigh number is denoted R_c^*, given by

$$R_c^* = \frac{r+(1-r)/\gamma}{r+(1-r)/\beta} R_c, \tag{2.12}$$

where R_c is the critical value of R. For the two-dimensional flows to be considered,

R_c^* is also a function of the non-dimensional cell width L. It takes its minimum value $R_{c\,\min}$ for a cell width $L = L_c$; these values correspond to the critical Rayleigh number and cell width for onset of convection in a system of infinite horizontal extent.

A measure of the amount of heat transferred vertically through the system is provided by the non-dimensional Nusselt number Nu. A first approximation for Nu, valid for slightly supercritical convection, is given by

$$Nu = 1 + \sigma\left(\frac{R^*}{R_c^*} - 1\right). \tag{2.13}$$

The parameter σ may be calculated by the method given in McKibbin & O'Sullivan (1981), where it was shown that for a general multilayered system, and also for a single layer with an open top, σ varies with cell width L.

3. The homogeneous anisotropic layer

Some results for a homogeneous anisotropic layer with a closed top are outlined in Kvernvold & Tyvand (1979). For a two-dimensional convection pattern with cell width L, the critical Rayleigh number R_c^* (where R^* is defined by (2.10)) is

$$R_c^* = \tfrac{1}{4}(\xi + L^2)(\eta + L^2)/\xi L^2. \tag{3.1}$$

The minimum value with respect to variation of L is given when

$$L = L_c = (\xi\eta)^{\frac{1}{4}}, \tag{3.2}$$

$$R_c^* = R_{c\,\min}^* = \tfrac{1}{4}(1 + (\eta/\xi)^{\frac{1}{2}})^2, \tag{3.3}$$

results which were first found by Epherre (1975). Note that $L_c > 1$ in the anisotropic modelling of layered porous media, since $\xi, \eta > 1$ from (2.8).

A first estimate for the Nusselt number Nu was provided by Kvernvold & Tyvand (1979) for the closed-top layer when $L = L_c$ (wavenumber $\alpha = \alpha_c$ in their paper) i.e. for a layer of infinite horizontal extent. They found that, for the preferred onset cell width $L = L_c$ given in (3.2), the parameter σ in the formula

$$Nu = 1 + \sigma\left(\frac{R^*}{R_{c\,\min}^*} - 1\right), \tag{3.4}$$

is independent of ξ and η and takes the value 2·0. From a new analysis made as part of the present study, it is found that σ is also independent of the cell width L, i.e. that σ always takes the value 2·0. So if an anisotropic layer with a closed top is bounded laterally by vertical insulating walls, thus providing a constraint on cell width, the critical Rayleigh number R_c^* is given by (3.1), and a first approximation for Nu by

$$Nu = 1 + 2\left(\frac{R^*}{R_c^*} - 1\right), \tag{3.5}$$

for all values of ξ, η and L. This result provides an addition to that given in McKibbin & O'Sullivan (1981) – it can now be stated that the coefficient σ, which for a multilayered or open-top configuration varies with cell width L, is in fact independent of L for a homogeneous layer, isotropic or anisotropic, with a closed top.

No simple expressions for $R_c^*(L)$, $R_{c\,\min}^*$, L_c and σ are available for the open-top case. From Kvernvold & Tyvand (1979), however, it may be deduced that $R_{c\,\min}^*$,

ξ/η	0·01	0·02	0·05	0·1	0·2	0·5	1·0
$R_{c\,min}$	10·6	6·16	3·18	2·04	1·38	0·895	0·686
$L_c/(\xi\eta)^{\frac{1}{4}}$	1·30	1·33	1·35	1·36	1·37	1·36	1·35
σ	2·94	3·00	2·95	2·80	2·55	2·19	1·95
ξ/η	1·0	2·0	5·0	10·0	20·0	50·0	100·0
$R_{c\,min}$	0·686	0·553	0·442	0·388	0·349	0·314	0·296
$L_c/(\xi\eta)^{\frac{1}{4}}$	1·35	1·33	1·29	1·24	1·20	1·14	1·11
σ	1·95	1·80	1·75	1·79	1·87	1·95	1·98

TABLE 1. Some values of $R^*_{c\,min}$, $L_c/(\xi\eta)^{\frac{1}{4}}$ and corresponding σ for a homogeneous anisotropic layer with an open top. All depend on ξ and η in the ratio ξ/η only.

$L_c/(\xi\eta)^{\frac{1}{4}}$ and σ all depend on ξ and η in the ratio ξ/η only – the different kinematic upper boundary condition does not alter this aspect of their analysis. Numerical calculations following an analysis similar to that for the closed top case verifies this. Some values of $R^*_{c\,min}$, $L_c/(\xi\eta)^{\frac{1}{4}}$ and corresponding σ for the open-top case are shown in table 1. (Wooding (1976) gave some values of $R^*_{c\,min}$ and L_c for the special case $\eta = 1$.) It should be noted that, unlike the closed-top case, σ varies with cell width L also.

If the homogeneous anisotropic porous layer is to be a suitable analogue for a multilayered system with a closed top, then as N becomes large, the values of $R^*_c(L)$, L_c and $R^*_{c\,min}$ should become close to those values given in (3.1)–(3.3), and $\sigma(L)$ close to the constant value 2·0. Similarly, for the open-top case, convergence to those values for a single anisotropic layer is required.

4. Results

In the homogeneous anisotropic model, convection occurs throughout the whole layer; using the distinction made by Masuoka *et al.* (1978) it can be said that 'large-scale' convection takes place. However, as noted by those authors and also by McKibbin & O'Sullivan (1980), for large non-homogeneities in permeability or conductivity in multilayered systems, it is possible that convection may begin in only some of the layers (those with larger permeability or smaller conductivity). Such motion is termed 'local' convection, and is almost confined to these active layers. Owing to continuity, however, some motion also takes place in the passive layers of small permeability or large conductivity.

If the multilayered system is to be modelled successfully by an anisotropic analogue, the local-convection type of motion should not appear as the number N of layers becomes large. Now, for most two-layer systems there is a tendency for local convection to occur as the ratios β, γ become much different from unity (these ratios correspond to the $1/\delta$, $1/\gamma$ of Masuoka *et al.*). An example of this is demonstrated in figure 1 (*a*), which shows values of R^*_c *vs.* L for the closed-top case $\beta = 0{\cdot}172$, $\gamma = 1{\cdot}0$ where all layer depths are equal ($r = 0{\cdot}5$), corresponding to effective anisotropy $\xi = 2{\cdot}0$, $\eta = 1{\cdot}0$. For $N = 2$, the cell width L_c (where $R^*_c = R^*_{c\,min}$) is significantly smaller than for $N \geqslant 4$, when the values of L_c are close to that for the corresponding homogeneous anisotropic layer. As N becomes larger, the values of R^*_c quickly approach the homogeneous values. Similarly, the values of parameter σ for each L approach the value 2·0 as N becomes large – this is shown in figure 1 (*b*). As explained in McKibbin

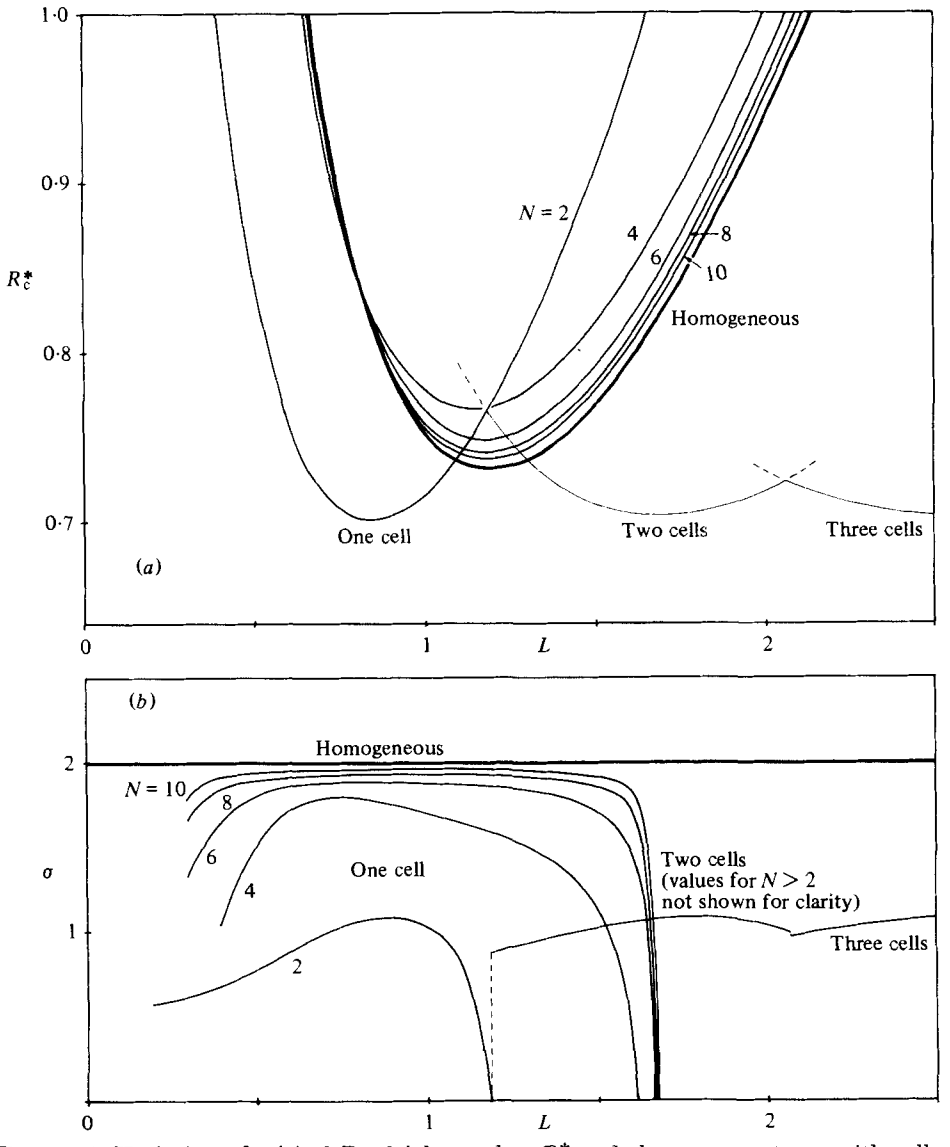

FIGURE 1. Variation of critical Rayleigh number R_c^* and slope parameter σ with cell width L for the case $\xi = 2{\cdot}0$, $\eta = 1{\cdot}0$, closed top, for number of layers $N = 2, 4, 6, 8, 10$ of equal depth ($r = 0{\cdot}5$) and for an equivalent homogeneous anisotropic layer. (*a*) R_c^* *vs.* L; (*b*) σ *vs.* L.

& O'Sullivan (1981) the values of σ for a layered system become zero at the value of L above which a two-cell flow becomes preferred. For $N \geqslant 4$, values of σ are given for a single cell only – those for larger numbers of cells may be deduced by suitable scaling of the graphs for a single cell. Streamlines for the cases $N = 2$, 4, 6 when $L = L_c$ are shown in figure 2, where comparison may be made with the convection pattern at onset in the homogeneous layer. The local ($N = 2$) and large-scale convection associated with the different numbers of layers is clearly seen.

By increasing either of the parameters ξ or η sufficiently, it can be shown that local convection will occur for both $N = 2$ *and* for a larger number of layers. For example,

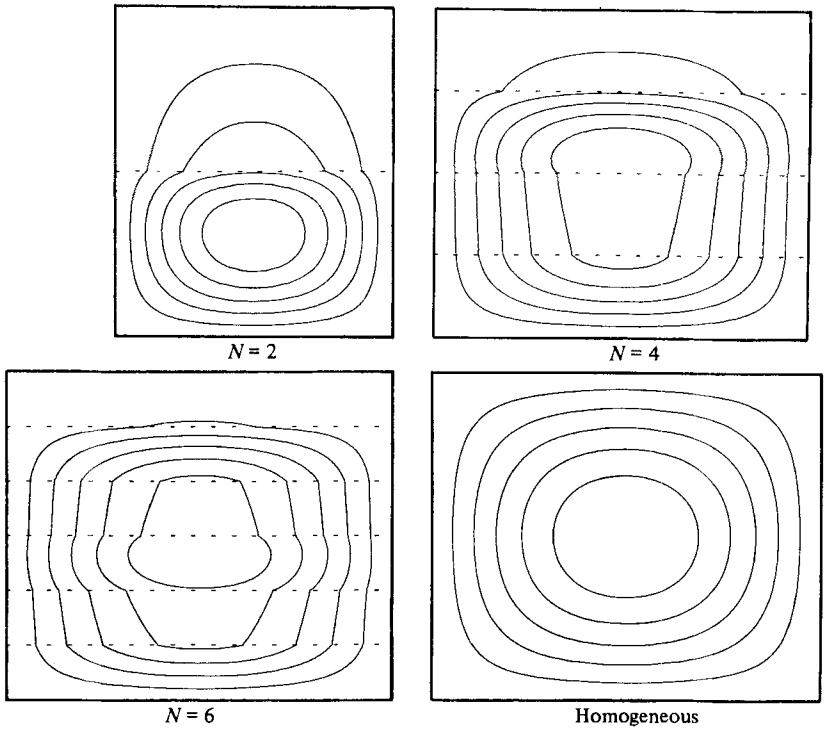

FIGURE 2. Streamlines of single cells at onset of convection in a laterally unbounded system for $\xi = 2{\cdot}0$, $\eta = 1{\cdot}0$, closed top, $r = 0{\cdot}5$, for $N = 2$ ($R^*_{c\,\min} = 0{\cdot}701$, $L_c = 0{\cdot}847$, $\sigma = 1{\cdot}07$), $N = 4$ (0·765, 1·15, 1·61), $N = 6$ (0·748, 1·17, 1·85) and a homogeneous layer (0·729, 1·19, 2·00).

if all layers have equal thickness and conductivity, local convection occurs when $\beta = 0{\cdot}01$ for both $N = 2$ and $N = 4$. Figure 3 gives the values of R^*_c *vs.* L for this case, while figure 4 shows streamlines for $N = 2$, 4, 6 and the homogeneous layer when $L = L_c$, all configurations having effective permeability anisotropy $\xi = 25{\cdot}5$. It will be shown that local convection is associated with still larger numbers of layers as ξ is increased further (see §6 below).

As noted by both Masuoka *et al.* (1978) and McKibbin & O'Sullivan (1980, 1981), some layered configurations (although only in certain small parameter ranges) result in two local minina for R_c (and hence R^*_c) as a function of cell width L. In particular, for some cases the smaller of the two minima corresponds to local convection while the larger corresponds to large-scale convection. Again taking $\eta = 1{\cdot}0$ (all layers of equal conductivity) the two-layer closed-top system where $r = 0{\cdot}2$, $\beta = 0{\cdot}025$ (giving $\xi = 7{\cdot}1$, $\eta = 1{\cdot}0$) exhibits such behaviour. For $N = 4, 6, \ldots$ however, there is only one minimum for $R^*_c(L)$, this corresponding to large-scale convection. Figure 5 shows how the preference in this configuration for local convection is associated only with the two-layer case, and vanishes for larger numbers of layers.

Systems with an open top (i.e. a constant-pressure upper-boundary condition) exhibit similar behaviour to those examples given above, as also do multilayered media where the permeability is uniform throughout, but conductivity varies from layer to layer. An example incorporating both types is shown in figure 6, where layer depths and permeabilities are all equal ($r = 0{\cdot}5$, $\beta = \xi = 1{\cdot}0$) and each system has an

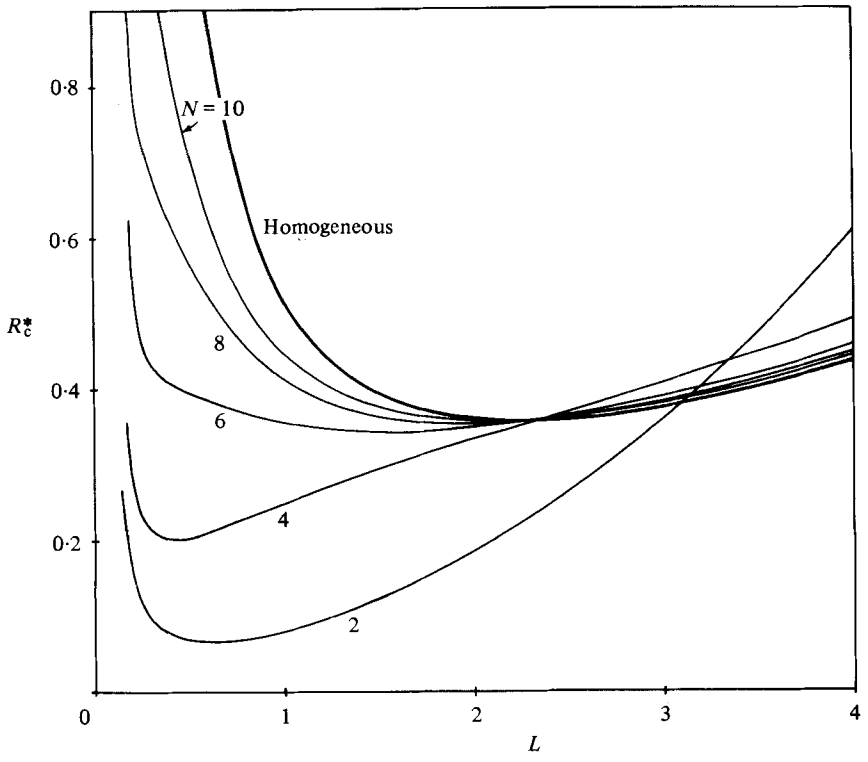

FIGURE 3. Variation of R_c^* with L for the case $\xi = 25{\cdot}5$, $\eta = 1{\cdot}0$, closed top, for layers of equal depth ($r = 0{\cdot}5$), and for a homogeneous layer.

open top. Figure 6(*a*) shows R_c^* *vs.* L for $\gamma = \gamma^- = 0{\cdot}0556$ and figure 6(*b*) for $\gamma = \gamma^+ = 18{\cdot}0$ – both values of γ give the same effective conductivity anisotropy $\eta = 5{\cdot}0$, but, as mentioned earlier, symmetry is not preserved because of the different types of upper- and lower-boundary conditions. The effect is seen only with the smaller numbers of layers, and, as N becomes large, the distinction tends to disappear as both systems model the homogeneous layer better. Streamlines at onset (when $L = L_c$) for $N = 2, 6$ are shown for both values of γ in figure 7, and may there be compared with the homogeneous-layer flow pattern.

5. Convergence

As shown by the examples above, for given ξ and η the homogeneous anisotropic layer models a layered system increasingly better as N becomes larger. Similarly, for a given number of layers N it is of interest to find out how well a homogeneous anisotropic medium models the layered system for various equivalent values of ξ and η. For the representative case $N = 8$, $r = 0{\cdot}5$, values of $R_{c\,\min}^*$ and L_c were calculated for $\xi, \eta = 1{\cdot}0, 2{\cdot}0, 5{\cdot}0, 10{\cdot}0$ and compared with the homogeneous values. Table 2 gives results for a closed-top system (using $\beta = \beta^-$, $\gamma = \gamma^-$) and table 3 gives those for the open-top case (using $\beta = \beta^+$, $\gamma = \gamma^+$). For each pair (ξ, η), the homogeneous value, the layered-system value and the percentage difference are given. As can be seen, convergence is generally better for ξ than for η, especially for $R_{c\,\min}^*$. This is related to the

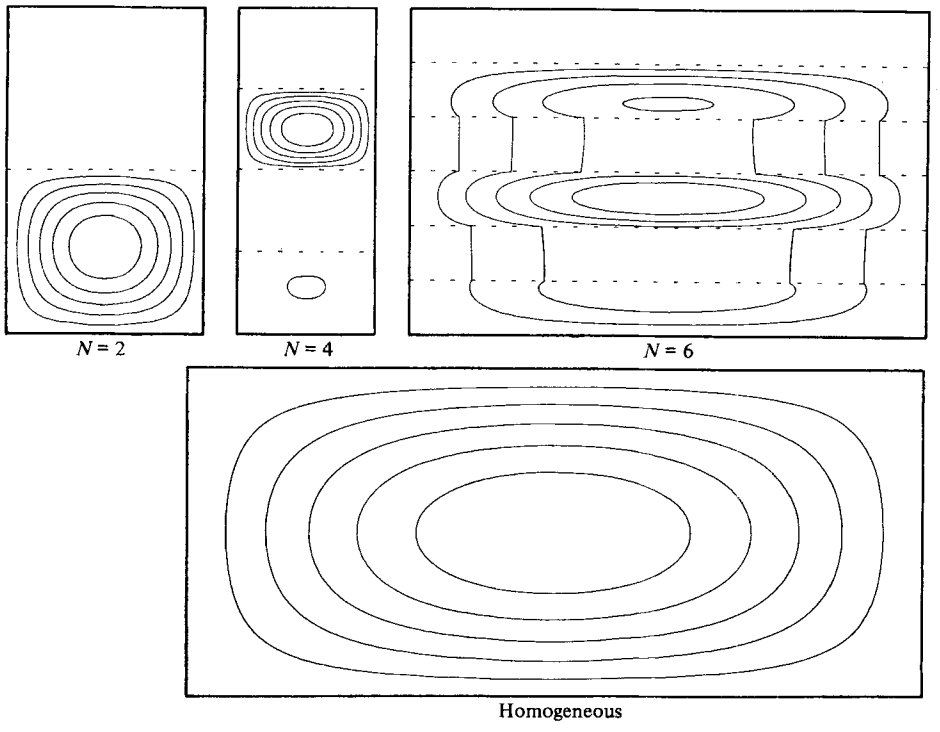

FIGURE 4. Streamlines at onset of convection in a laterally unbounded system for $\xi = 25{\cdot}5$, $\eta = 1{\cdot}0$, closed top, $r = 0{\cdot}5$ for $N = 2$ ($R^*_{c\,\mathrm{min}} = 0{\cdot}065$, $L_c = 0{\cdot}601$, $\sigma = 0{\cdot}53$), $N = 4$ (0·202, 0·422, 0·26), $N = 6$ (0·345, 1·57, 1·34) and a homogeneous layer (0·359, 2·25, 2·00).

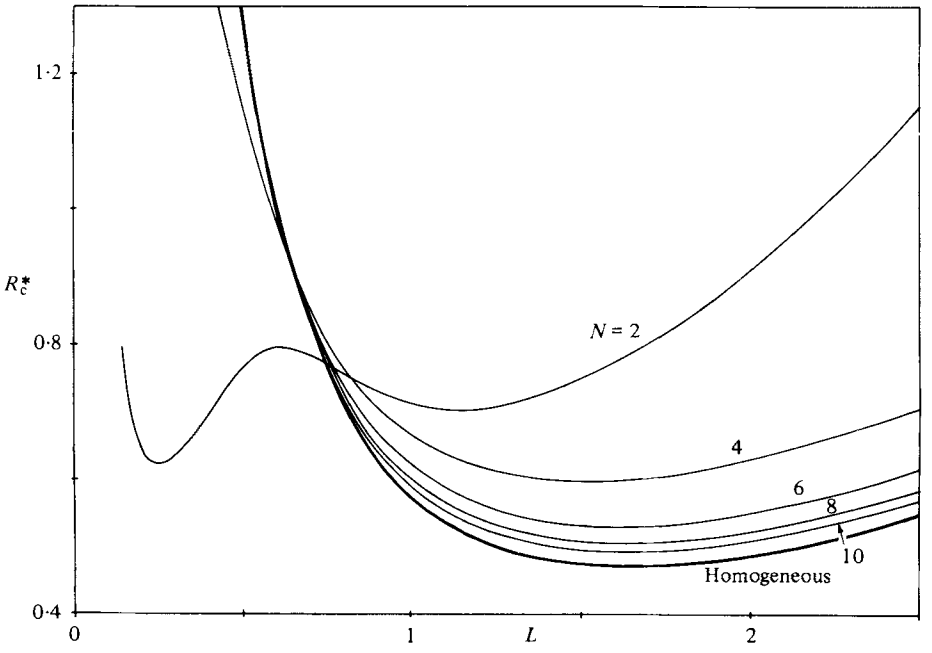

FIGURE 5. Variation of R_c^* with L for the case $\xi = 7{\cdot}1$, $\eta = 1{\cdot}0$, $r = 0{\cdot}2$, closed top (giving two minima for $N = 2$).

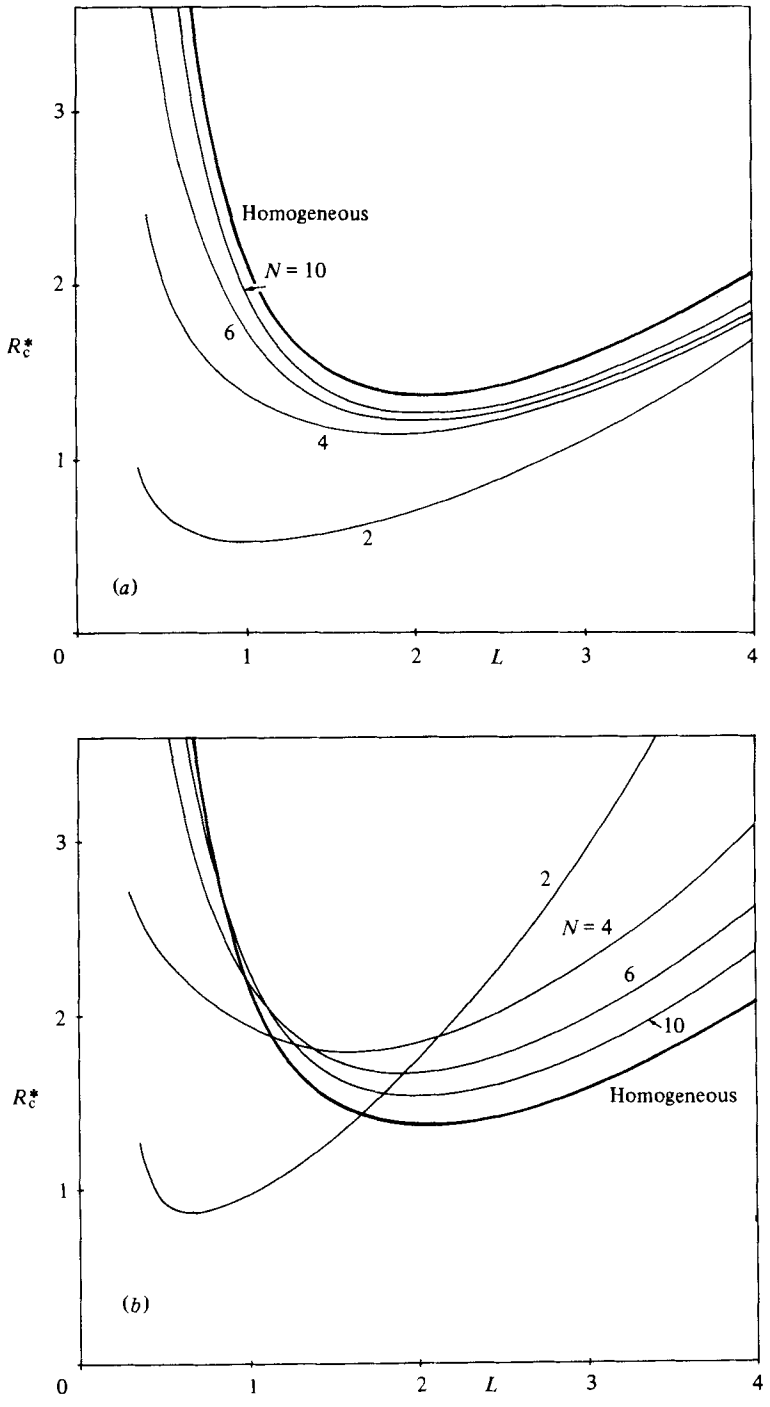

FIGURE 6. Variation of R_c^* with L for the open-top case $\xi = 1{\cdot}0$, $\eta = 5{\cdot}0$, $r = 0{\cdot}5$. (*a*) $\gamma = \gamma^- = 0{\cdot}0556$; (*b*) $\gamma = \gamma^+ = 18{\cdot}0$.

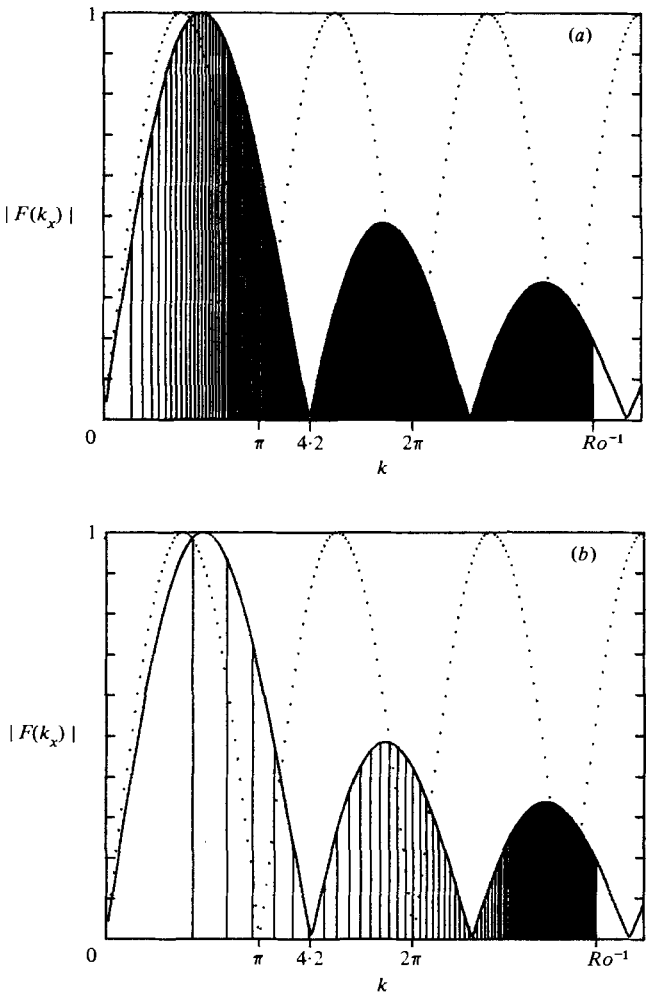

FIGURE 2. Normalized Fourier transforms, $|F_1(k_x)|/|F_{1\max}|$ and $|F_2(k_x)|/|F_{2\max}|$, of $\partial f_i/\partial x$ for the cylindrical ridge $f_1(x)$ (solid) and the top-hat ridge $f_2(x)$ (dotted) respectively. Vertical lines denote $|F_1(k_x)|/|F_{1\max}|$ for k_n^-, $n = 1, 2, 3, \ldots$, for (*a*) $Ro = 0{\cdot}1$, $H = 10$ and (*b*) $Ro = 0{\cdot}1$, $H = 1$.

2 shows that as H decreases, the largest-amplitude modes are eliminated. A similar trend for the low wavenumbers is obtained by fixing H and decreasing Ro. This suggests that for small Ro, in a fluid of finite depth, or for small H, the inertial waves are weak, as shown by Stewartson & Cheng (1979).

Qualitative comparisons are made of observed three-dimensional surfaces of constant phase and those predicted by Lighthill's theory. The far-field, three-dimensional surfaces of constant phase, are given in parametric form by

$$x = \frac{\Phi}{k_x}\left[1 + k_x^2 \frac{1 - Ro^2 k_x^2}{k_x^2 + k_y^2}\right], \tag{2.16a}$$

$$y = \Phi k_y \frac{1 - Ro^2 k_x^2}{k_x^2 + k_y^2}, \tag{2.16b}$$

$$z = \pm \frac{\Phi}{Ro\, k_x} \frac{(1 - Ro^2 k_x^2)^{\frac{3}{2}}}{(k_x^2 + k_y^2)^{\frac{1}{2}}}, \tag{2.16c}$$

ξ	1·0		2·0		5·0		10·0	
η	$R^*_{c\,min}$	L_c	$R^*_{c\,min}$	L_c	$R^*_{c\,min}$	L_c	$R^*_{c\,min}$	L_c
	1·000	1·000	0·729	1·189	0·523	1·495	0·433	1·778
1·0	1·000	1·000	0·740	1·182	0·534	1·461	0·439	1·691
	0·0	0·0	+1·6	−0·6	+2·1	−2·3	+1·4	−4·9
	1·457	1·189	1·000	1·414	0·666	1·778	0·524	2·115
2·0	1·475	1·169	1·069	1·398	0·731	1·762	0·580	2·090
	+1·2	−1·7	+6·9	−1·2	+9·8	−0·9	+10·7	−1·1
	2·618	1·495	1·666	1·778	1·000	2·236	0·729	2·659
5·0	2·630	1·412	1·793	1·717	1·118	2·199	0·827	2·632
	+0·5	−5·5	+7·6	−3·4	+11·8	−1·7	+13·4	−1·0
	4·331	1·778	2·618	2·115	1·457	2·659	1·000	3·162
10·0	4·248	1·573	2·780	1·971	1·621	2·575	1·135	3·106
	−1·9	−11·5	+6·2	−6·8	+11·3	−3·2	+13·5	−1·8

TABLE 2. Comparison of the values of $R^*_{c\,min}$ and L_c for an 8-layer model with a closed top and layers of equal depth ($r = 0{\cdot}5$), with those values for an equivalent homogeneous anisotropic layer. For each pair of values (ξ, η) the values given are (i) homogeneous value, (ii) layered-system value, (iii) percentage difference $((\text{ii})/(\text{i}) - 1) \times 100$. The ratios $\beta = \beta^-$ and $\gamma = \gamma^-$ are used.

ξ	1·0		2·0		5·0		10·0	
η	$R^*_{c\,min}$	L_c	$R^*_{c\,min}$	L_c	$R^*_{c\,min}$	L_c	$R^*_{c\,min}$	L_c
	0·686	1·351	0·553	1·581	0·442	1·922	0·388	2·209
1·0	0·686	1·351	0·554	1·533	0·439	1·854	0·382	2·108
	0·0	0·0	+0·2	−3·0	−0·7	−3·6	−1·6	−4·6
	0·895	1·619	0·686	1·910	0·520	2·349	0·442	2·719
2·0	0·995	1·576	0·787	1·802	0·593	2·210	0·500	2·564
	+11·2	−2·7	+14·7	−5·7	+14·0	−5·9	+13·0	−5·7
	1·379	2·042	0·985	2·426	0·686	3·020	0·553	3·536
5·0	1·595	1·964	1·198	2·257	0·833	2·807	0·664	3·296
	+15·7	−3·8	+21·6	−7·0	+21·3	−7·1	+20·0	−6·8
	2·041	2·422	1·379	2·889	0·895	3·622	0·686	4·271
10·0	2·378	2·289	1·714	2·651	1·117	3·338	0·849	3·954
	+16·5	−5·5	+24·3	−8·2	+24·9	−7·8	+23·6	−7·4

TABLE 3. As for table 2, but for an open top. The ratios $\beta = \beta^+$ and $\gamma = \gamma^+$ are used.

matching with the anisotropic model. Now, in the 'alternating-layer' model, all the R_i will be equal if

$$\frac{R_2}{R_1} = \frac{(K_2/K_1)\,d_2^2/d_1^2}{k_2^2/k_1^2}\left(= \frac{\beta(1-r)^2}{\gamma^2 r^2}\right) = 1. \tag{5.1}$$

An example where this is so is given by $\beta = 0{\cdot}05$, $\gamma = 1{\cdot}0$, $r = 0{\cdot}183$ (giving $\xi = 3{\cdot}7$, $\eta = 1{\cdot}0$), results for which are given in figures 8 and 9 for a closed-top system. Figure 8 shows variation of R_c^* with L, and certainly shows a lack of tendency towards local

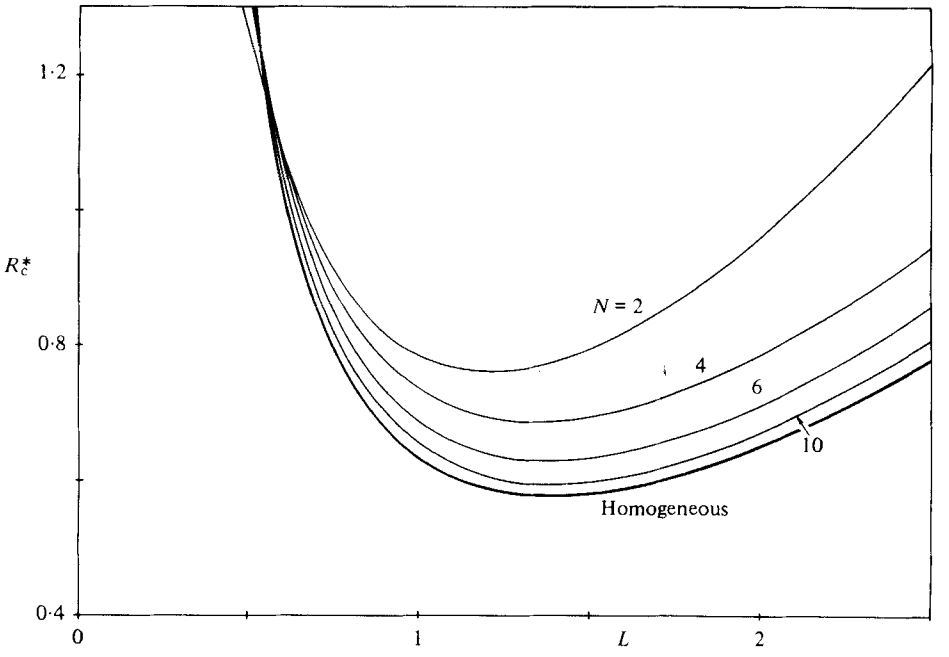

FIGURE 8. Variation of R_c^* with L for the case $\xi = 3{\cdot}70$, $\eta = 1{\cdot}0$, closed top, $r = 0{\cdot}183$, where all layer Rayleigh numbers R_i are equal.

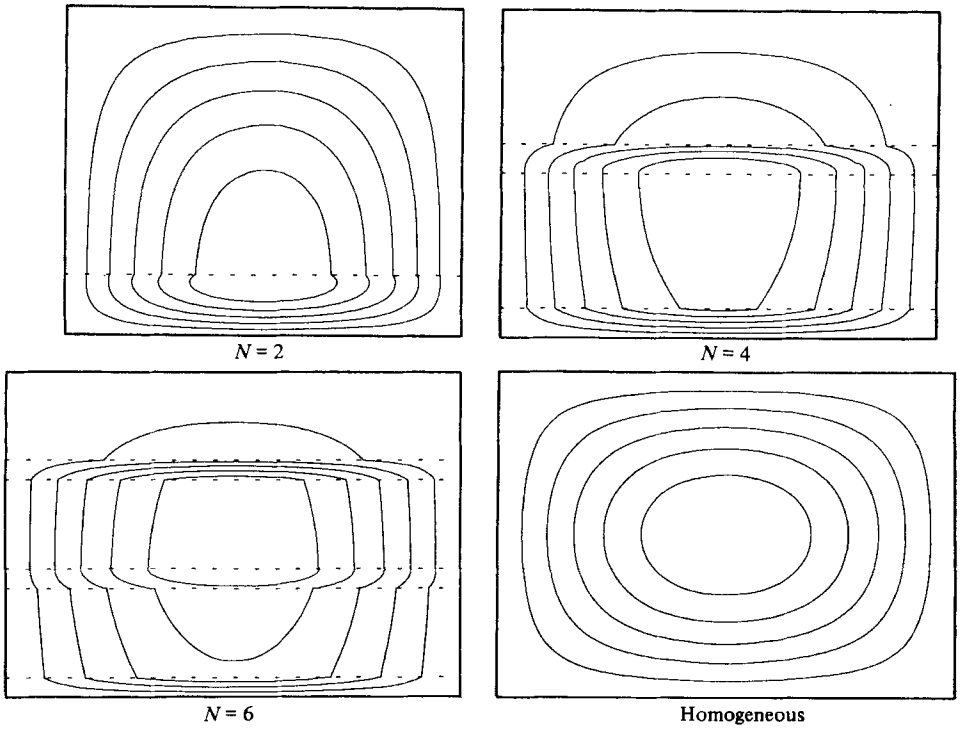

FIGURE 9. Streamlines at onset of convection in a laterally unbounded system for $\xi = 3{\cdot}70$, $\eta = 1{\cdot}0$, closed top, $r = 0{\cdot}183$ for $N = 2$ ($R^*_{c\,\min} = 0{\cdot}761$, $L_c = 1{\cdot}20$, $\sigma = 1{\cdot}87$), $N = 4$ (0·690, 1·33, 1·25), $N = 6$ (0·631, 1·37, 1·53) and a homogeneous layer (0·578, 1·39, 2·00).

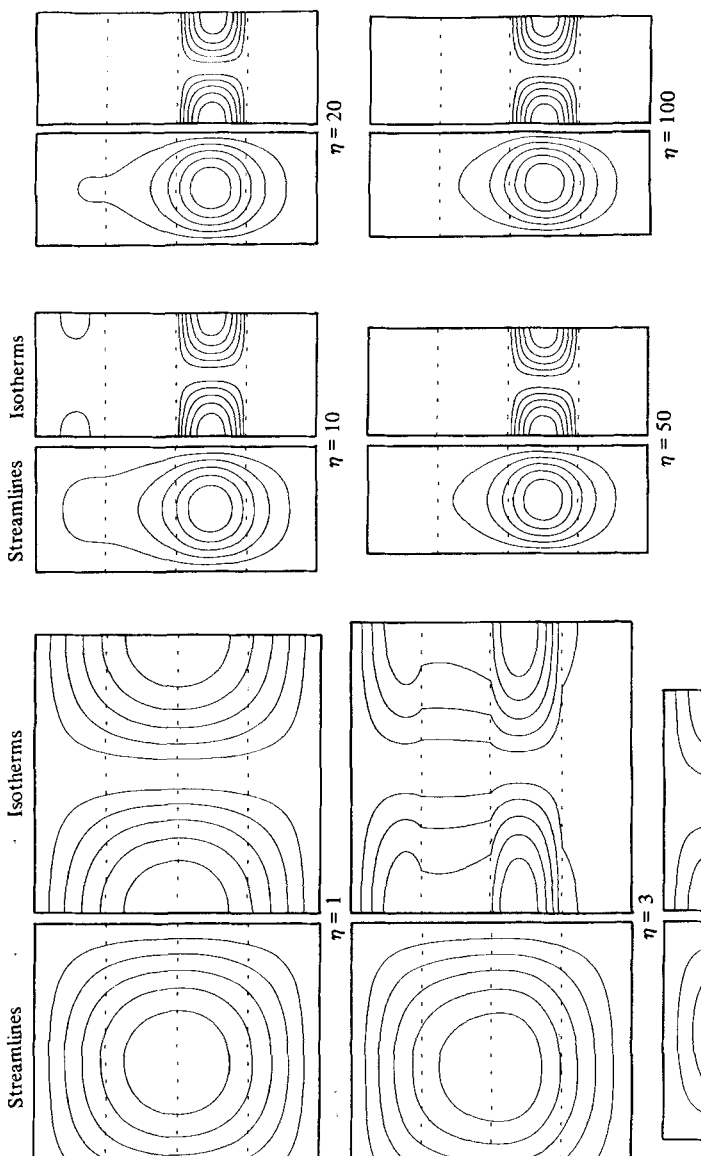

FIGURE 10. Streamlines and isotherms (departures from the conduction solution) at onset of convection in a laterally unbounded system for $\xi = 1{\cdot}0$, closed top, $N = 4$, $r = 0{\cdot}5$ for $\eta = 1{\cdot}0$ ($R^*_{c\,\min} = 1{\cdot}0$, $L_c = 1{\cdot}0$, $\sigma = 2{\cdot}00$), $\eta = 3{\cdot}0$ (1·85, 1·05, 2·02), $\eta = 5{\cdot}0$ (2·35, 0·79, 1·46), $\eta = 10{\cdot}0$ (2·59, 0·45, 0·72), $\eta = 20{\cdot}0$ (2·64, 0·41, 0·67), $\eta = 50{\cdot}0$ (2·66, 0·39, 0·65) and $\eta = 100{\cdot}0$ (2·67, 0·38, 0·64).

d_2^2/d_1^2	K_2/K_1 = 1·0	0·5	0·2	0·1	0·05
		(*a*) ξ			
1·0	1·00	1·13	1·80	3·03	5·51
2·0	1·00	1·12	1·78	2·97	5·38
5·0	1·00	1·11	1·68	2·73	4·85
10·0	1·00	1·09	1·58	2·48	4·30
20·0	1·00	1·07	1·48	2·21	3·70

(*b*) % deviation $R^*_{c\,min}$

0	+1·3	−1·4	−18	−42	0	+0·6	+2·4	+3·4	+3·4
0	+1·7	+6·5	−1·4	−28	0	+0·6	+2·9	+4·7	+5·8
0	+1·1	+9·8	+19	+6·8	0	+0·6	+3·2	+5·9	+8·2
0	+0·3	+7·5	+20	+33	0	+0·5	+3·0	+6·0	+9·1
0	−0·3	+4·3	+15	+34	0	+0·3	+2·5	+5·6	+9·2

(*c*) % deviation L_c

0	−4·7	−24	−44	−57	0	−0·2	−1·0	−2·4	−5·0
0	−1·7	−18	−43	−63	0	−0·1	−0·9	−1·8	−3·5
0	+1·9	−6·2	−21	−71	0	−0·1	−0·5	−1·1	−2·0
0	+3·2	−0·6	−9·7	−24	0	−0·1	−0·4	−0·9	−1·4
0	+3·6	+2·7	−3·5	−14	0	−0·0	−0·2	−0·5	−1·1

(*d*) % deviation σ

0	−5·0	−40	−63	−70	0	−1·5	−6·4	−10·5	−14·6
0	−0·7	−25	−66	−77	0	−1·6	−7·5	−12·9	−18·1
0	+2·8	−4·0	−36	−84	0	−1·4	−8·1	−15·1	−21·9
0	+5·7	+1·7	−6·5	−43	0	−1·2	−7·7	−15·4	−23·3
0	+8·2	+6·0	+0·6	−6·7	0	−0·9	−6·6	−14·5	−23·3
		$N = 2$					$N = 6$	

TABLE 4. Values of ξ and percentage differences of $R^*_{c\,min}$, L_c and σ from the homogeneous values for two- and six-layer models of alternating layers, with a closed top and uniform conductivity. For each pair of ratios (K_2/K_1, d_2^2/d_1^2) values are given for (*a*) ξ and the percentage differences for (*b*) $R^*_{c\,min}$, (*c*) L_c and (*d*) σ. On the main diagonal of each table, all layer Rayleigh numbers R_i are equal.

convection for all N, in contrast to those examples given in figures 1–7. The streamlines at onset when $L = L_c$ for $N = 2, 4, 6$ and the homogeneous layer in figure 9 show the broad similarity in cell shape.

The results above suggest that $R_1 = R_2$ may give the best agreement with anisotropy, at least for the case $N = 2$. Further calculations were carried out to find whether this criterion (that all the R_i be equal) has relevance for $N = 2$ and also for larger numbers of layers. Values of $R^*_{c\,min}$, L_c and σ were found for the closed-top cases $N = 2$ and $N = 6$ when all layer conductivities are equal ($k_2/k_1 = 1{\cdot}0$) for a variety of values of K_2/K_1 and d_2^2/d_1^2, and the differences from the anisotropic values are presented in table 4. It shows that, contrary to initial expectation, the percentage deviations in $R^*_{c\,min}$ are greatest on the main diagonal, where all the R_i are equal. The values of L_c tend to improve in agreement with increasing d_2^2/d_1^2 (decreasing ξ), especially for $N = 6$, but do not attain optimum values on the main diagonal. The factor $K_i d_i^2/k_i^2$ thus appears not to be of major relevance. The last case given in figures 8 and 9 does not therefore give the best agreement with anisotropy – however, it still remains a representative case where local convection does not occur.

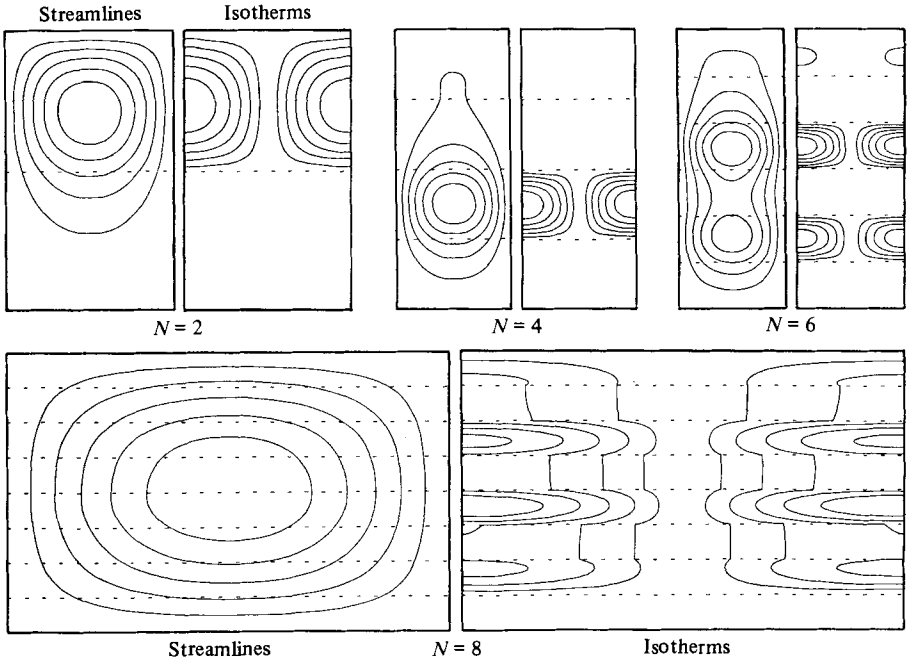

FIGURE 11. Streamlines and isotherms at onset of convection in a laterally unbounded system for $\xi = 1{\cdot}0$, $\eta = 20{\cdot}0$, closed top, $r = 0{\cdot}5$ for $N = 2$ ($R^*_{c\,\min} = 0{\cdot}847$, $L_c = 0{\cdot}60$, $\sigma = 2{\cdot}25$), $N = 4$ (2·64, 0·41, 0·67), $N = 6$ (5·54, 0·38, 1·08), $N = 8$ (6·98, 1·58, 1·79). Corresponding values for the equivalent homogeneous layer are (7·49, 2·11, 2·0).

The onset criterion for local convection in a multilayered system thus seems dependent on the more active layers in the configuration (i.e. those layers in which greatest flow occurs). Figure 4 shows examples of active and passive layers for $N = 2$ and 4. As ξ or η becomes large, the most active layer tends to become that which is both most centrally situated and for which R_i is largest. Even though the local Rayleigh number in the topmost or bottom layer may have an equal R_i, the presence of the horizontal boundary causes the layer to become less active than that nearest the centre. (This of course does not apply to the case $N = 2$.) A further example to illustrate this is given in figure 10, showing the closed-top case $N = 4$, where all layers have equal depth and permeability – increasing η (decreasing $\gamma = \gamma^-$) causes the cell width L_c to decrease as convection is confined more and more to layer 2 (although the local Rayleigh number R_4 for the top layer is the same as R_2). Both the streamlines and isotherms (departure from the conduction temperature distribution) become markedly concentrated in layer 2.

Examination of further examples given in figure 11 helps to broaden some of these aspects. The case of equal layer depths and uniform permeability is still considered, but N is now varied while thermal anisotropy is fixed ($\eta = 20{\cdot}0$, $\gamma = 0{\cdot}0128$). The stabilizing influence of the upper boundary is clearly demonstrated: little recirculation takes place in the topmost layer, provided other active layers exist. Local convection occurs up to $N = 6$, where there is recirculation in both the second and fourth layers. For $N = 8$ large-scale convection occurs, with a streamline pattern close to that of the homogeneous case.

The layers will thus never be equally active in the onset of convection as long as

there are unequal influences of the top and bottom boundaries on the different layers. However the difference in activity between the top/bottom layer and internal layers with the same R_i is much larger than between the internal layers themselves. These boundary effects also reduce the significance of the factor $K_i d_i^2/k_i^2$.

6. A sufficient condition for onset of local convection in a closed-top system

Values of $R^*_{c\,\min}$ presented in the examples above, for a layered system with a closed top and with no tendency towards local convection, all exceed the critical value for its anisotropic equivalent, namely $R^*_c = R^*_{c\,\min} = \frac{1}{4}(1+(\eta/\xi)^{\frac{1}{2}})^2$. This seems to be a general lower limit; genuinely large-scale convection cannot start for R^* below this value in a laterally unbounded layered system. On the other hand, local convection may occur in any layer for which R_i exceeds $4\pi^2$; this value of R_i for any $i = 1, 2, \ldots, N$ is thus an upper limit for local convection, because the possibility of motion outside the active layer(s) acts in a destabilizing manner. (For instance the value of R_1 at onset in the case $N = 4$ of figure 4 is $R_1 = 2{\cdot}55\pi^2$). Analogously, thermal interaction between two Newtonian fluid layers, transmitted through a solid layer, is known to act in a destabilizing manner (Gershuni & Zhukhovotskii 1976, p. 43).

Now, when R^* reaches the value $R^* = \frac{1}{4}(1+(\eta/\xi)^{\frac{1}{2}})^2$, either R_1 or R_2 (representative layer Rayleigh numbers for all layers in the alternating-layer configuration) may have reached $4\pi^2$, so that local convection has started in the system. This gives a condition for a class of media for which local convection *must* be preferred. (It may also occur outside this range). A *sufficient* condition for local convection in the closed top case is found by combining the inequality $\max\{R_1, R_2\} > 4\pi^2$ with the equation $R^* = \frac{1}{4}(1+(\eta/\xi)^{\frac{1}{2}})^2$ to arrive at the inequality:

$$\left[\left(\frac{r+(1-r)/\beta}{r+(1-r)/\gamma}\right)^{\frac{1}{2}} + \left(\frac{r+(1-r)\gamma}{r+(1-r)\beta}\right)^{\frac{1}{2}}\right]^2 > \frac{r+(1-r)/\gamma}{r^2} N^2 \min\left\{1, \frac{\gamma^2 r^2}{\beta(1-r)^2}\right\}. \tag{6.1}$$

The two terms in the minimum bracket correspond to the criteria $R_1 > 4\pi^2$, $R_2 > 4\pi^2$ respectively. (From (5.1), the two are equal if $R_1 = R_2$.)

The condition (6.1) was tested for all the closed-top cases presented so far. It was found to be satisfied for the examples in figure 4 for $N = 2$ and 4, for those in figure 10 for $\eta \geqslant 10{\cdot}0$ and in figure 11 for $N = 2$ and 4, all of which show convection of local type.

It may be easily shown from (6.1) that, if one of β or $1/\gamma \to 0$ while the other remains finite, the sufficiency condition is satisfied for any arbitrary N provided the diminishing value of β or $1/\gamma$ (as the case may be) is taken small enough. This verifies that if alternate layers are either completely impermeable or infinitely conducting, local convection must occur.

As mentioned above, the tendency towards local convection in a layered system with given ξ, η decreases with increasing numbers of layers – this is also now reflected in the inequality (6.1). But it is better illustrated by considering the onset criteria for varying ξ or η. As these parameters are increased from the value 1·0, the values of $R^*_{c\,\min}$, L_c and σ (the Nusselt-number slope parameter in the formula $Nu = 1+\sigma(R^*/R^*_c - 1)$) for a homogeneous layer are approximated better and better by

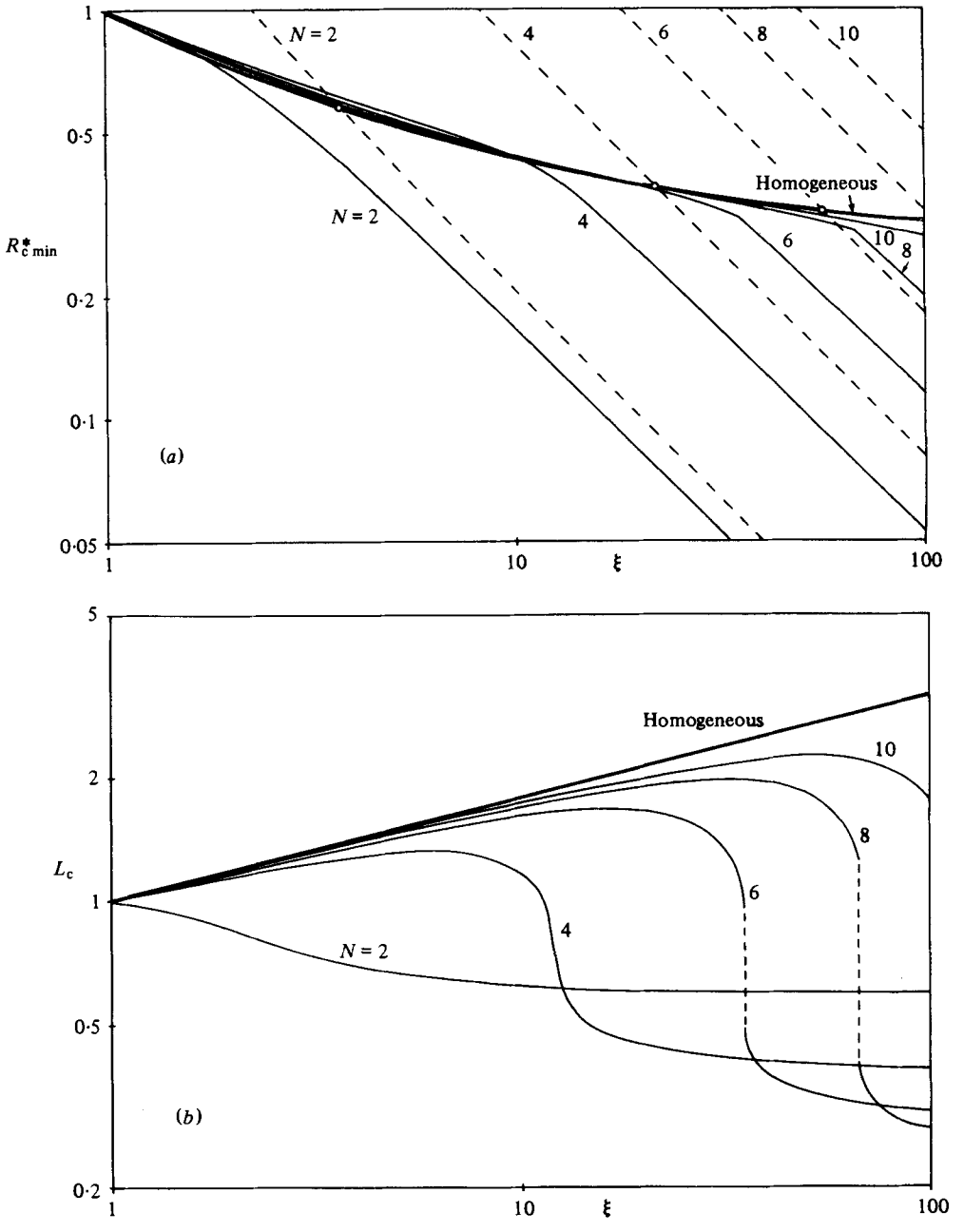

FIGURE 12 (*a*, *b*). Caption on p. 334.

larger numbers of strata in the equivalent layered systems. In the results given below, only the case of equal layer depths in a closed-top system are considered.

Figure 12 shows the variation of $R^*_{c\,min}$, L_c and corresponding σ values with ξ ($\beta = \beta^-$) when $\eta = 1{\cdot}0$, for $N = 2, 4, 6, 8, 10$ and the homogeneous anisotropic layer. For $N \geqslant 4$ there is a marked transition over a very small range of ξ from large-scale convection throughout the whole system to local convection within the more per-

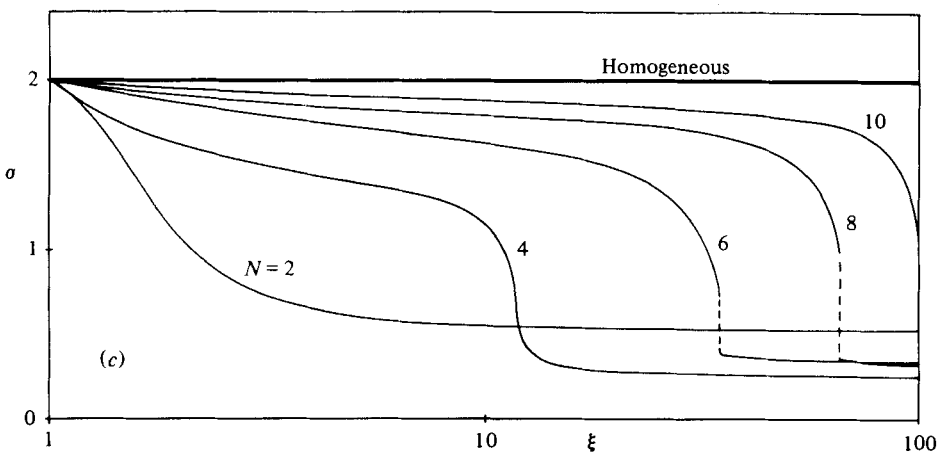

FIGURE 12. Variation of $R^*_{c\,min}$, L_c and corresponding values of σ with ξ for the case of uniform conductivity ($\eta = 1{\cdot}0$), closed top and equal layer depths ($r = 0{\cdot}5$). (*a*) $R^*_{c\,min}$ *vs.* ξ: – – –, values of R^*_c where $R_1 = 4\pi^2$; (*b*) L_c *vs.* ξ; (*c*) σ *vs.* ξ.

meable layers, the transition occurring for larger values of ξ as N increases. To the right of the transition region for each N, the values of $R^*_{c\,min}$ decrease in such a way that

$$\xi R^*_{c\,min} = \frac{\rho_a g c \alpha K_H d \Delta T}{4\pi^2 \nu k},$$

is nearly constant i.e. for local convection a Rayleigh number based on the effective horizontal permeability has a critical value that is nearly independent of permeability ratio ξ.

Figure 12(*b*) shows that there is a tendency towards local convection in a system with two layers of equal thickness. The L_c and σ curves for $N = 2$ never approach the homogeneous curve, since even the starting slopes at $\xi = 1{\cdot}0$ are markedly different. Greater numbers of layers give large-scale convection when ξ is not too large. After the transition to local convection, L_c is small and decreases with increasing N. The small cell width for local convection may be interpreted as a tendency to form near-square cells in the active layer, as noted by McKibbin & O'Sullivan (1980, p. 389).

Similar variation of $R^*_{c\,min}$, L_c and σ with η when $\xi = 1{\cdot}0$ is shown in figure 13. The same transition behaviour as for the previous case is evident. To the right of each transition region, the values of $R^*_{c\,min}$ become asymptotically constant with increasing η for each N.

Comparison of figures 12 and 13 show that the anisotropy description is better for ξ than for η – the transition regions for given N in figure 12 lie to the right of those in figure 13. The transition values of ξ are approximately twice those of η for the same N. This is related to the different powers in the ratio $K_i d_i^2/k_i^2$, as already mentioned.

The sufficiency condition for local convection has been included in figures 12(*a*) and 13(*a*). The curves where $R_1 = 4\pi^2$ (corresponding to $R^* = N^2/(\xi + (\xi^2 - \xi)^{\frac{1}{2}})$, from (2.5) and (2.9)) are shown as dashed lines in figure 12(*a*). For a given N, inequality (6.1) is satisfied for ξ greater than that value (marked with a ring) where the dashed line crosses the homogeneous-layer line (representing $R^*_{c\,min} = \frac{1}{4}(1 + (\eta/\xi)^{\frac{1}{3}})^2$. The figure confirms that $R_1 < 4\pi^2$ at onset of local convection.

The dashed curves indicate more, however. The distance between them and the

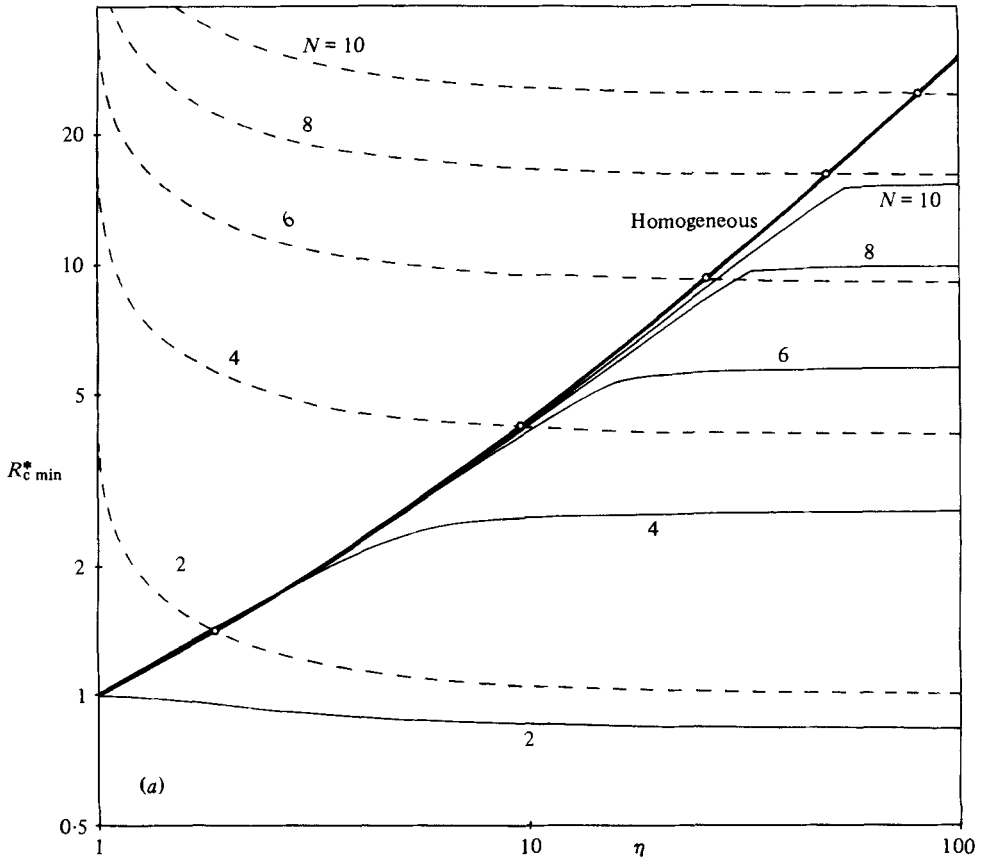

FIGURE 13 (*a*). Caption on p. 336.

correct curves are about half as large (relatively, on the log–log scales used) for $N = 2$ as for $N = 4, 6, 8 \ldots$ in the range of local convection. This is not accidental. First, none of the lines for $R_1 = 4\pi^2$ are asymptotes for the correct curves – they assume the same kinematic boundary conditions as for the asymptotic case (impermeable) but not the same thermal boundary conditions. For $N = 2$, local convection is restricted to the first layer, where one thermal boundary condition is correct. For $N \geqslant 4$, this is not so, since the first layer is not the most active. Accordingly, for $N = 2$, *three* out of the four boundary conditions are asymptotically correct (referring to the case of impermeable, perfectly conducting boundaries with critical local Rayleigh number equal to $4\pi^2$) while for $N \geqslant 4$ only *two* out of four conditions are asymptotically correct.

Similar comments may be applied to figure 13(*a*), where the dashed lines are the curves for $R_2 = 4\pi^2$ (corresponding to $R^* = N^2(\eta - (\eta^2 - \eta)^{\frac{1}{2}})^2$). By comparing the upper-bound transition points (rings in figures 12(*a*) and 13(*a*)) predicted by the sufficiency condition, these turn out to have values about half as large for η as for ξ.

7. The heat flux

The mean vertical heat flux is measured by the Nusselt number Nu, which is approximated for slightly supercritical flow by (2.13). Nu depends on the parameter σ,

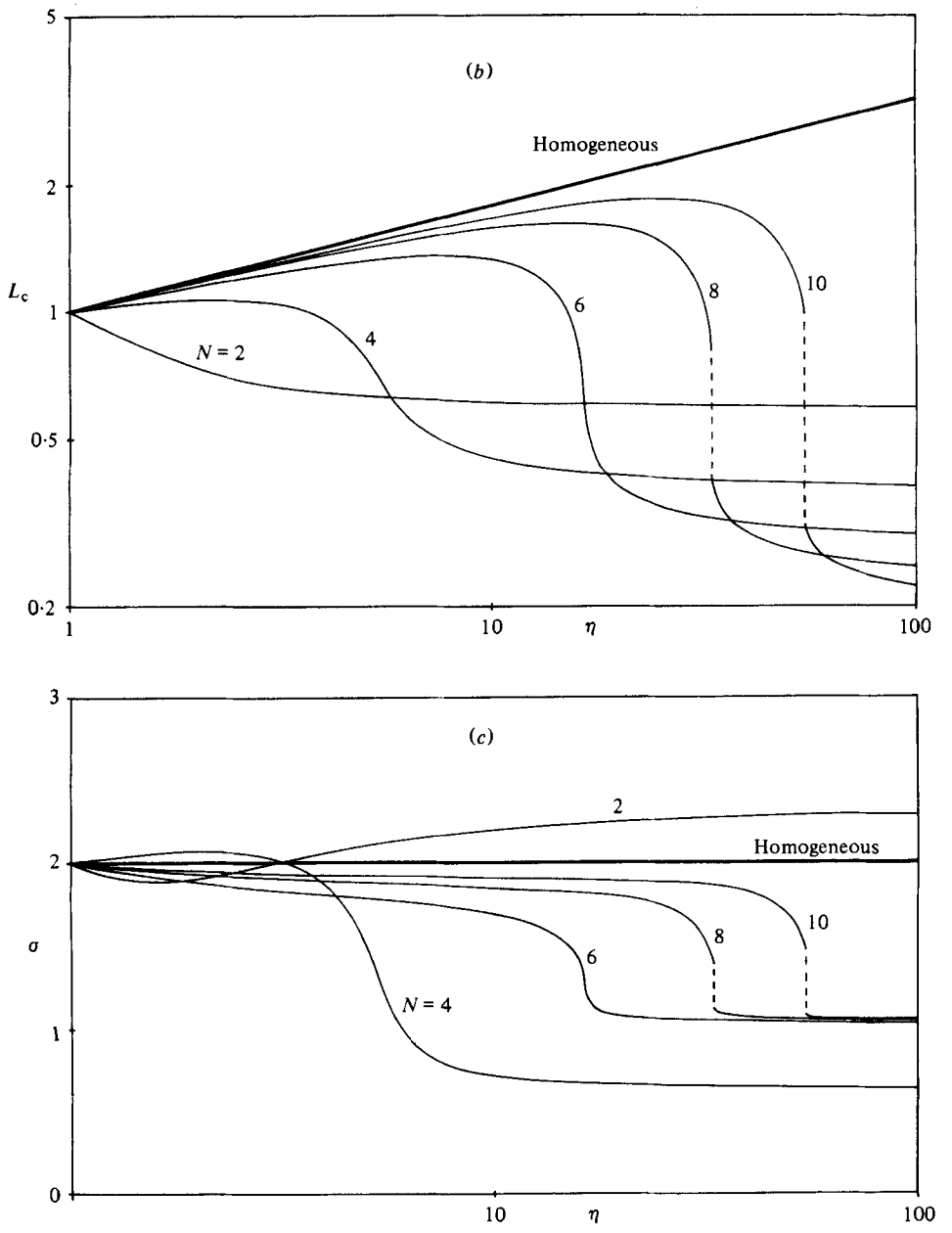

FIGURE 13. Variation of $R^*_{c\,min}$, L_c and corresponding values of σ for the case of uniform permeability ($\xi = 1{\cdot}0$), closed top and equal layer depths ($r = 0{\cdot}5$). (*a*) $R^*_{c\,min}$ *vs.* η: – – –, values of R^*_c where $R_2 = 4\pi^2$; (*b*) L_c *vs.* η; (*c*) σ *vs.* η.

the slope of the graph of Nu *vs.* R^*/R^*_c. For a homogeneous anisotropic layer with a closed top the value of σ is 2·0 and is independent of ξ and η, and also of cell width L. For a layered system σ varies with the configuration and boundary conditions. The values of σ corresponding to $R^*_c = R^*_{c\,min}$, $L = L_c$ for the closed-top configurations given in figures 12(*a*, *b*) and 13(*a*, *b*) are shown in figures 12(*c*), 13(*c*).

The values of σ show the same transition regions as $R^*_{c\,\min}$ and L_c, with a marked decrease in value at the transitions. As ξ or η becomes very large, the values of σ become asymptotically constant.

It should be noted that the values of σ associated with a local type of convection (except for the case $\xi = 1{\cdot}0$, $N = 2$ in figure 13) are much smaller than for large-scale convection. The rate of heat transfer for slightly supercritical flows is thus greater when the motion is large-scale (as noted by McKibbin & O'Sullivan 1981). When local convection occurs, there may be almost immobile internal fluid layers where most of the heat is to be transported by conduction. This strongly impedes the heat transport unless all nearly stagnant layers have large conductivity. In large-scale convection, nearly stagnant internal layers do not exist.

For systems where conductivity is uniform ($\eta = 1{\cdot}0$) as shown in figure 12, the layered-system values of σ are all less than the homogeneous anisotropy value of 2·0. The less-permeable layers are constrained to transfer heat mainly by conduction – as ξ becomes large almost-immobile internal layers appear and the convective heat transfer is reduced.

For the case of uniform permeability ($\xi = 1{\cdot}0$), shown in figure 13, σ may be larger than 2·0 for small N. In particular, for $N = 2$, the less-conductive upper layer has a concentration of convection. This combines with the high conductivity of the lower layer to produce large heat transfer (and $\sigma > 2{\cdot}0$ for large η). For $N = 4$ and $\eta < 3{\cdot}2$ convection is reasonably strong in both of the less-conductive layers (see figure 10 for $\eta = 3{\cdot}0$) and $\sigma > 2{\cdot}0$. For $\eta > 3{\cdot}2$ however the upper layer becomes less active and the heat transfer drops, with $\sigma < 2{\cdot}0$. The transition towards local convection begins. In figure 10 the progression as η increases for $N = 4$ can be studied. The case $\eta = 5{\cdot}0$ is interesting as it is just in the middle of the transition region (see figure 13*b*), and the flow in this case is intermediate between large-scale and local convection. As η increases further, local convection appears in the second layer; the uppermost layer becomes more and more inactive, leading to small heat transfer. Figure 11 indicates that the top layer is the only layer of small conductivity that will be inactivized (for $N > 2$) as η increases. Accordingly, the heat-insulating effect of this inactivization decreases as the thickness of the uppermost layer decreases (i.e. as N increases). This explains why $N = 4$ has the smallest asymptotic value for σ.

Existing theory is able to give some information about the heat transport in layered porous media for larger supercritical Rayleigh numbers. Results for homogeneous anisotropic layers are given by Kvernvold & Tyvand (1979, figure 2). The Nusselt number as a function of R/R_c depends on the ratio ξ/η. The effects of anisotropy are not great, but Nu is always larger for any value $\xi/\eta = b$, where $b < 1$, than for $\xi/\eta = 1/b > 1$ (assuming R/R_c fixed). This result suggests that, for layered systems, layering in conductivity ($\eta > 1$) causes more rapid growth in heat transport with increasing R than does permeability layering ($\xi > 1$).

8. Conclusions

Thermal convection in a multilayered porous medium has been investigated, with the purpose of comparison with asymptotic limits of homogeneous anisotropy. This comparison offers a simplified description of layering, as well as a physical understanding of anisotropy. The case of alternating layers gives good convergence as the

number of layers becomes large. Anisotropy models the occurrence of large-scale convection only. For a given number of layers, there may be a sudden breakdown of this anisotropic modelling at the appearance of local convection, which consists mainly of flow in single layers, for a local Rayleigh number somewhat below $4\pi^2$.

From wave theory (Brekhovskikh 1960) it is known that anisotropic modelling of layered media accounts for interfacial refraction but not for interfacial reflection phenomena. Similarly, anisotropic modelling of convection accounts for interfacial refraction of streamlines and/or isotherms, but not for recirculations constrained by interfaces.

The present results indicate that a curved flow in a periodically layered porous medium can be modelled in terms of homogeneous anisotropy for most practical purposes, provided the length scale of the flow is larger than the layering period. Calculations for $N = 2$ show that anisotropic modelling may be useful also for aperiodic layering, provided the flow is of large-scale type.

The average continuum description is fundamental to the theory of flows through porous media (Bear 1972, p. 19). In a general context, the present model is distinguished as it offers a quantitative analysis of the accuracy of the average continuum description. Usually such an analysis is impracticable as it requires calculation of the Newtonian fluid flow in the irregular pores. The difference here is the existence of two distinct levels of average continuum description: the lower level of layering and the higher level of anisotropy. An analysis of the accuracy of the higher-level description may thus be performed in terms of the lower-level description.

REFERENCES

Bear, J. 1972 *Dynamics of Fluids in Porous Media.* Elsevier.

Brekhovskikh, L. M. 1960 *Waves in Layered Media.* Academic.

Castinel, G. & Combarnous, M. 1974 Critère d'apparition de la convection naturelle dans une couche poreuse anisotrope horizontale. *C.r. hebd. Séanc. Acad. Sci. Paris* B **278**, 701–704.

Cheng, P. 1978 Heat transfer in geothermal systems. *Adv. Heat Transfer* **14**, 1–105.

Combarnous, M. A. & Bories, S. A. 1975 Hydrothermal convection in saturated porous media. *Adv. Hydrosci.* **10**, 231–307.

Donaldson, I. G. 1962 Temperature gradients in the upper layers of the earth's crust due to convective water flows. *J. Geophys. Res.* **67**, 3449–3459.

Epherre, J. F. 1975 Critère d'apparition de la convection naturelle dans une couche poreuse anisotrope. *Rev. Gén. Thermique* **168**, 949–950.

Gershuni, G. Z. & Zhukhovitskii, E. M. 1976 Convective stability of incompressible fluids. Jerusalem: Keter. (Originally publ. in Russian, 1972, Nauka.)

Green, T. & Freehill, R. L. 1969 Marginal stability in inhomogeneous porous media. *J. Appl. Phys.* **40**, 1759–1762.

Kvernvold, O. & Tyvand, P. A. 1979 Nonlinear thermal convection in anisotropic porous media. *J. Fluid Mech.* **90**, 609–624.

Marcus, H. & Evenson, D. E. 1961 Directional permeability in anisotropic porous media. *Water Resources Center Contrib.* no. 31, Hydrology Laboratory, University of California, Berkeley.

Masuoka, T., Katsuhara, T., Nakazono, Y. & Isozaki, S. 1978 Onset of convection and flow patterns in a porous layer of two different media. *Heat Transfer–Japanese Res.* **7**, 39–52.

McKibbin, R. & O'Sullivan, M. J. 1980 Onset of convection in a layered porous medium heated from below. *J. Fluid Mech.* **96**, 375–393.

McKibbin, R. & O'Sullivan, M. J. 1981 Heat transfer in a layered porous medium heated from below. *J. Fluid Mech.* **111**, 141–173.

MORANVILLE, M. B., KESSLER, D. P. & GREENKORN, R. A. 1977*a* Directional dispersion coefficients in anisotropic porous media. *Ind. Engng Chem. Fund.* **16**, 327–332.

MORANVILLE, M. B., KESSLER, D. P. & GREENKORN, R. A. 1977*b* Dispersion in layered porous media. *A.I.Ch.E. J.* **23**, 786–794.

RIBANDO, R. & TORRANCE, K. E. 1976 Natural convection in a porous medium: effects of confinement, variable permeability, and thermal boundary conditions. *Trans. A.S.M.E.* C, *J. Heat Transfer* **98**, 42–48.

TYVAND, P. A. 1980 Approximate formulae for the dispersion coefficients of layered porous media. *A.I.Ch.E. J.* **26**, 513–517.

WOODING, R. A. 1976 Influence of anisotropy and variable viscosity upon convection in a heated saturated porous layer. *New Zealand D.S.I.R. Tech. Rep.* no. 55.

ZEBIB, A. & KASSOY, D. R. 1977 Onset of natural convection in a box of water-saturated porous media with large temperature variation. *Phys. Fluids* **20**, 4–9.